agronomy

MDPI

Article

The Isolation and Identification of a New Pathogen Causing Sunflower Disk Rot in China

Jianfeng Yang [1], Yujie Wang [2], Shenghua Shi [3], Haoyu Li [2], Wenbing Zhang [1], Mandela Elorm Addrah [1], Jian Zhang [1] and Jun Zhao [1,*]

[1] College of Horticulture and Plant Protection, Inner Mongolia Agricultural University, Hohhot 010019, China; jianfengyang89@126.com (J.Y.); zhangwenbing@imau.edu.cn (W.Z.); mdl@emails.imau.edu.cn (M.E.A.); zhj19890128@imau.edu.cn (J.Z.)
[2] Bayannur Modern Agriculture and Animal Husbandry Development Center, Bayannur 015000, China; yj08202064@163.com (Y.W.)
[3] Inner Mongolia Bayannur Agricultural and Livestock Product Quality and Safety Center, Bayannur 015000, China
* Correspondence: zhaojun@imau.edu.cn

Abstract: Sunflower (*Helianthus annuus*) is an important oil crop, ranking behind soybean, peanut, and rapeseed in terms of planting area in China. Throughout its cultivation, sunflower is susceptible to various diseases that can significantly reduce its seed yield. Among them, *Fusarium* species pose a major threat to numerous crops. The accurate identification of *Fusarium* species responsible for specific diseases is crucial for developing effective control measures. In Inner Mongolia, sunflower disk rot (SDR) has been observed in various sunflower fields, with an average infection rate of approximately 8.50%. The infection rate can reach up to 11.67% in certain highly susceptible cultivars. Samples of diseased sunflower receptacles were collected from different locations, and Koch's postulates were employed to identify the causal agent. The results confirmed *Fusarium verticillioides* as the pathogen responsible for SDR. Fungicide toxicity tests were conducted, screening six fungicides for efficacy against *F. verticillioides*. Fludioxonil and Flutolanil were identified as the most effective, with EC50 values of 0.05 μg/mL (R = 0.9825) and 0.96 μg/mL (R = 0.9964), respectively. This is the first report of SDR caused by *F. verticillioides*, and it will alert sunflower researchers to include SDR in the disease list, so as to control sunflower diseases with integrated management strategies successfully.

Keywords: sunflower; *Fusarium verticillioides*; new disease; fungicide screenings

check for updates

Citation: Yang, J.; Wang, Y.; Shi, S.; Li, H.; Zhang, W.; Addrah, M.E.; Zhang, J.; Zhao, J. The Isolation and Identification of a New Pathogen Causing Sunflower Disk Rot in China. *Agronomy* **2024**, *14*, 1486. https://doi.org/10.3390/agronomy14071486

Academic Editor: Ivo Toševski

Received: 27 May 2024
Revised: 5 July 2024
Accepted: 5 July 2024
Published: 9 July 2024

Copyright: © 2024 by the authors. Licensee MDPI, Basel, Switzerland. This article is an open access article distributed under the terms and conditions of the Creative Commons Attribution (CC BY) license (https://creativecommons.org/licenses/by/4.0/).

1. Introduction

Sunflower (*Helianthus annuus* L.) ranks as the fourth largest oil crop globally and is primarily cultivated in Eastern Europe, China, Turkey, and other regions [1,2]. According to the Food and Agriculture Organization of the United Nations (FAO), the global planting area for sunflower reached 27.3 million hectares, with a total yield of 56.1 million tons in 2021. In China, the Ministry of Agriculture and Rural Affairs (http://www.moa.gov.cn/URL (accessed on 18 April 2022)) reported a sunflower planting area of 0.92 million hectares in 2022. Inner Mongolia is the largest sunflower-producing region in China, accounting for approximately 0.45 million hectares [3].

Currently, over 30 diseases affecting sunflower have been reported worldwide. Among these, three types of sunflower head rot significantly impact sunflower yield. Bacterial head rot is caused by *Pectobacterium carotovorum* and *P. atrosepticum* [4,5]. Rhizopus head rot is attributed to *Rhizopus stolonifer*, *R. oryzae* (syn. *R. arrhizus*), and *R. microsporus* [6,7]. Sclerotinia head rot is caused by *Sclerotinia sclerotiorum* [8]. Distinguishing between the symptoms of head rot caused by different fungal pathogens, namely *Rhizopus* and *Sclerotinia* species, can be challenging due to their similar manifestations, whereas head rot caused by bacteria presents distinct symptoms.

In 2020 and 2021, a disease survey was conducted across four major sunflower-growing regions in Inner Mongolia (Bayannur, Erdos, Ulanqab, and Baotou) during the R1 to R8 growth stages. The symptoms observed were similar to sunflower head rot caused by *Rhizopus* spp. Characteristic symptoms included circular dark brown lesions at the border of the bracts and on the backside of the receptacle. Lesion sizes on the receptacle ranged from 7.5 to 9.6 cm in length and from 5.5 to 8.6 cm in width. Under conditions of high precipitation, the lesions expanded rapidly, leading to the wilting of bracts and soft rot of the receptacle. White hyphae were consistently observed at the infection sites.

Fusarium spp. are significant pathogens responsible for various diseases affecting roots, stems, and leaves, including wilt, root rot, stem rot, and top rot. These pathogens lead to yield losses and reduced quality in crops, vegetables, fruit trees, and medicinal plants. *Fusarium verticillioides* (*F. verticillioides*) is notably the causal agent of root rot in tobacco [9], and it has recently been identified as a pathogen causing stem rot in cucumber [10] and rhizome rot in ginger [11]. Additionally, *F. verticillioides* can infect a range of crucial crops such as rice [12], maize [13], sorghum [14], corn [15], cotton [16], etc.

In order to identify the pathogen causing sunflower disk rot (SDR), Koch's postulates combined with a molecular technique were performed. PCR amplification using universal and specific primers for ITS, Tef1a, and rpb1 were conducted, and we constructed a phylogenetic tree to analyze the taxonomic status of the isolates using the multigene joint tandem technique. The growth rate of the mycelium was measured to screen for effective fungicides to control the isolated strains. The results obtained in this study are the first report of the causal agent causing SDR, and this will enrich the sunflower disease list and alert researchers to pay attention to this new disease.

2. Materials and Methods

2.1. Isolation and Culture

The seven SDR samples were collected from different fields in Guyang county (110°21′16″ E, 41°12′50″ N), BaoTou city, Inner Mongolia. All samples were packed in paper bags and brought back to the laboratory for pathogen isolation. The boundary tissues of the lesions were cut into 3~5 mm slices, surface sterilized with 5% sodium hypochlorite for 1 min, and then rinsed three times with sterile distilled water and briefly dried. The sterilized slices were placed on water agar (Agar, 20 gr/L, SIGMA-A9915, Shanghai, China) plates (five pierces per plate) and cultured for two days at 25 °C in an incubator (BIOBASE, BJPX-M150, Jinan, China). Mycelia surrounding the disinfected tissues were carefully excised with a sterilized needle, and pure cultures were obtained from single spores picked after serial dilutions on WA medium.

For pathogen identification, the morphological characteristics of the isolates were meticulously documented. These characteristics were observed and documented using an electron microscope (OLYMPUS, Chongqing, China). The colony morphology and color of the pure cultures were recorded after 7 days of incubation at 25 °C on potato dextrose agar (PDA) plates (containing 46 g/L, Hopebio, Yantai, China).

2.2. DNA Extraction, PCR Amplification, and DNA Sequencing

Pure isolates were cultured for 5 days on potato dextrose agar (PDA) medium. Fresh mycelium was then harvested from the plates for DNA extraction using the CTAB method [17]. The extracted DNA's quality was assessed on 1.2% agarose gel. To enhance our understanding of the higher-level phylogeny of Fusarium, we sequenced partial ITS (Internal Transcribed Spacer), RPB1 (DNA-dependent RNA polymerase II largest subunit), and Tef-1alpha (Translation elongation factor 1 alpha) genes from the fungi. For amplification, we employed primers ITS1 (5′-TCCGTAGGTGAACCTGCGG-3′) and ITS4 (5′-TCCTCCGCTTATTGA-TATGC-3′) [18], EF-1 (5′-ATGGGTAAGGA(A/G)-GACAAGAC-3′) and EF-2 (5′-GGA(G/A)GTACCAGT(G/C)ATCATGTT-3′) [19], RPB1-F1α (5′-CAYAARGARTCYATGATGGGWC-3′), and RPB1-G2 (5′-GTCATYTGDGTDGCDG GYTCDCC-3′) [20]. Each 25 µL reaction mixture contained 0.5 µL Taq DNA polymerase,

2.5 µL Taq buffer (2.5 mM), 2 µL dNTPs (2.5 mM each), 1 µL of each primer (10 pm each), and 50 ng genomic DNA. The cycling parameters included an initial denaturation step at 94 °C for 5 min, followed by 35 cycles at 94 °C for 40 s, 55/56 °C for 40 s, 72 °C for 40 s, and a final extension at 72 °C for 10 min. The annealing temperatures were set at 55 °C for ITS and 56 °C for Tef-1α and RPB1, respectively. PCR products were purified using a PCR product purification kit (Life Technologies, Carlsbad, CA, USA) and submitted to Beijing Hooseen Biotechnology Co., Ltd. for sequencing. The obtained sequences were compared with those of related species retrieved from GenBank (Table 1). ABI files were initially analyzed using MEGA 7.0 to filter out sequences with single peaks and clear peak patterns.

However, due to the presence of numerous misidentified strains and low-quality sequences that required filtering, the screened sequence range needed to be compared using BLAST from the NCBI. Subsequently, two gene sequences related to *Fusarium* were downloaded from the GenBank database (Table 1). The downloaded sequences, along with those obtained in this study, were batch processed using EditSeq in Lasergene 7.1. Multiple sequence alignment was performed using Clustal × 2.1. The GTR + I + G nucleotide substitution model was selected to account for rate heterogeneity among sites. Maximum Likelihood (ML) branching support was estimated through bootstrap analysis with 1000 pseudo-replicates using the specified model parameters. The phylogenetic tree was constructed using MEGA 7.0 software, employing the Maximum Likelihood method [21].

Table 1. Genebank ID number of gene sequences of different *Fusarium* Species from the NCBI.

Number	Taxon	Voucher Information	Genebank ID	
			TEF-1a	RPB1
001	*Fusarium duoseptatum*	CBS 102026	MH484987	MH484896
002	*Fusarium microconidium*	CBS 119843	MN120759	MN120721
003	*Fusarium proliferatum*	NRRL 62905	KU171727	KU171687
004	*Fusarium ussurianum*	NRRL 45681	FJ240301	KM361648
005	*Fusarium redolens*	NRRL 22901	KU171728	MT409432
006	*Fusarium verticillioides*	NRRL 25115	JF740741	HM347183
007	*Fusarium verticillioides*	NRRL 22172	MW401964	MW402497
008	*Fusarium verticillioides*	NRRL 54997	KC808228	KC808308
009	*Fusarium oxysporum*	NRRL 62545	KC808222	KC808305
010	*Fusarium acuminatum*	NRRL 45994	GQ505432	KC808324
011	*Fusarium keratoplasticum*	NRRL 25391	DQ246860	KC808311
012	*Fusarium petroliphilum*	NRRL 54988	KC808210	KC808287
013	*Fusarium falciforme*	NRRL 32778	DQ247088	KC808315
014	*Fusarium solani*	NRRL 32492	DQ246990	EU329584
015	*Verticillium dahliae*	Le1340	GU461623	——

2.3. Pathogenicity Test

To assess the pathogenicity of the isolates, a conidial suspension produced on wheat bran medium (15 days) was adjusted to a concentration of 5×10^6 spores/mL for inoculation on leaves, stems, and roots. Inoculated plants were obtained by sowing three seeds of LD5009 (provided by Kafry Technology Co., Ltd., Beijing, China) in pots (13 cm height × 13 cm diameter) containing a mixture of nutrient soil and field soil (1:5, v/v). These pots were kept in a growth chamber maintained at 25 to 28 °C with 70% relative humidity and a 12 h photoperiod. At the V8 stage (after 7 weeks of cultivation), sunflower leaves and stems were surface sterilized with 75% alcohol. Subsequently, 20 µL of conidial suspension (5×10^6 spores/mL) was inoculated using a hypodermic needle. For root inoculation, inoculation was performed at the V4 stage (after 3 weeks of cultivation), and 100 µL of conidial suspension (5×10^6 spores/mL) was poured into each pot, with sterilized water used as a blank control. The experiment was repeated three times.

The pathogenicity of the isolates on sunflower flower disks was evaluated in the field. At the R-5 stage of LD5009, a 100 mL conidial suspension (5×10^6 spores/mL) was injected into the backside of the flower disk using a sterile syringe. Three infection sites, equally

distributed on the backside of the flower disk, were established as replicates. The inoculated flower disks were covered with a dark plastic bag overnight to maintain moisture. Seven days post inoculation, the disease lesions were recorded, and their sizes were precisely measured.

2.4. Re-Isolation of the Pathogens on Seeds

When the sunflowers reached maturity, 1/8 of the disk was used to collect seeds for pathogen detection. For fungal isolation from sunflower seeds, 100 seeds were randomly selected and cracked open to obtain the inner seed. Surface sterilization of the sunflower seeds was performed before placing them on freshly prepared PDA medium, followed by drying in a laminar flow hood. Ten seeds were placed randomly on each Petri dish and incubated at 25 ± 2 °C in a dark chamber for 7 days. The number of seeds with fungal colonies was counted, and the contamination ratio was calculated. Fungal colonies were then transferred to new PDA plates for purification and morphological identification. Molecular characterization of the isolates was performed as described in Section 2.2.

2.5. Fungicide Sensitivity Evaluation

In this experiment, a total of six fungicides combined with five different concentrations were established. Detailed information on the treatments is provided in Table 2. Each concentration was replicated five times, with plates lacking fungicide serving as controls. The effects of each fungicide on inhibiting the mycelial growth of the tested isolates were assessed following the method outlined by Chen [22]. Briefly, PDA plugs were excised from the colony edges of the tested isolate and inoculated upside down in the center of plates containing various concentrations of the fungicide under investigation. After seven days of incubation at 25 °C, colony diameters were measured using the cross method, and the inhibition rate of mycelial growth was calculated using the following formula. The inhibitory effects of the different fungicides on isolate growth were compared, and the half-maximal effective concentration value (EC50) was determined following the approach described by Addrah et al. [23].:

Growth inhibition rate (%) = (control colony diameter-treated colony diameter)/control colony diameter) × 100.

The logarithm of the concentration (X) and the percentage probability value (Y) of inhibition effects on colony growth was calculated. The virulence regression equation, correlation coefficient, and EC50 value for each fungicide against the isolates were obtained using the least-squares method [24].

Table 2. Information on the six fungicides used in the study.

Fungicide Name	Dosage Form	Manufacturer Information
Tebuconazole · dimetachlone	70% WG	Wilda Chemical Co., Ltd., Hangzhou, China
Pyraclostrobine	25% EC	BASF (China) Co., Ltd., Shanghai, China
Iprodione	500 g/L SC	Suzhou Fumeishi Plant Protector Co., Ltd., Suzhou, China
Hymexazol	98% WP	Lvheng Biotechnology Co., Ltd., Jinan, China
Flutolanil	42.4% SC	BASF (China) Co., Ltd., Nantong, China
Fludioxonil	25 g/L FS	Syngenta Nantong Crop Protection Co., Ltd., Nantong, China

Notes: WG, water-dispersible granules; EC, emulsifiable concentrate; SC, aqueous suspension concentrate; WP, wettable powder; FS. suspension seed coating agent.

3. Results

3.1. Symptoms of Sunflower Disk Rot (SDR)

In 2021, SDR was observed at the R6 stage of sunflower cultivation in Inner Mongolia, China. Initially, the margins of the bracts were infected, displaying brown, irregular lesions, which subsequently expanded to other parts of the bracts. Concentric dark brown lesions were also evident on the backside of the flower disk (Figure 1a–c). Tissues beneath the

lesions on the flower disk exhibited rot, contributing to the enlargement of the lesions at the infection sites (Figure 1a). Following infection, the bracts of sunflowers wilted, and the flower disks began to deteriorate prematurely. The average disease incidence was estimated to range from 8.5% to 11.67% in the surveyed fields.

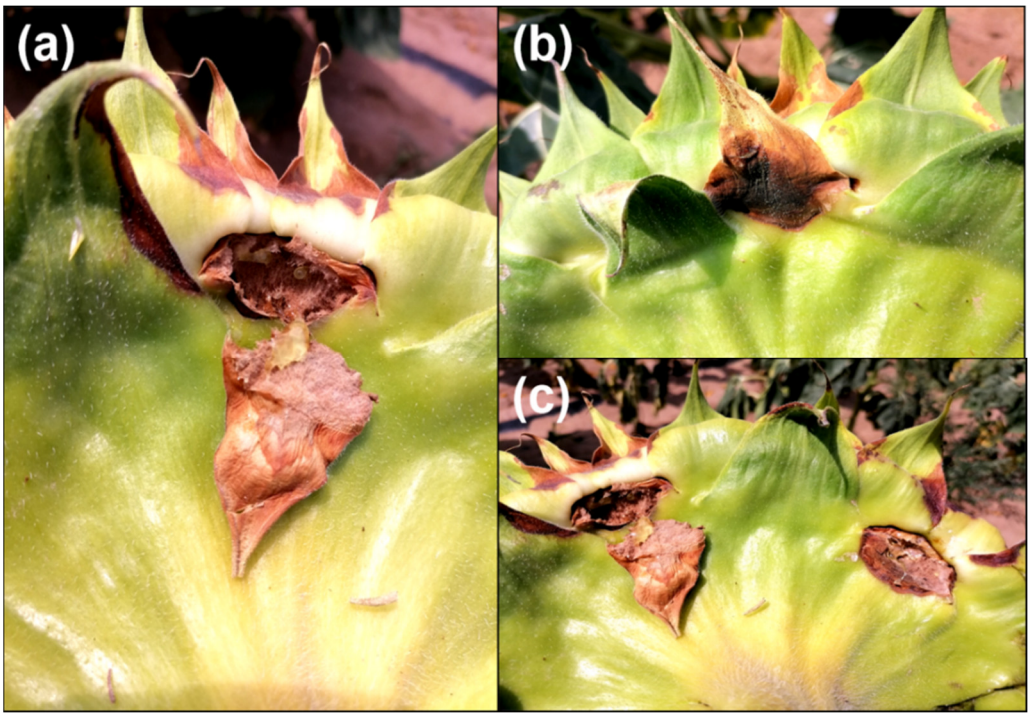

Figure 1. Symptoms of sunflower disk rot (SDR) in the field. (**a**) Symptoms on the margin of the sunflower bracts; (**b**) symptoms on sunflower bracts; (**c**) symptoms of simultaneous infection of multiple locations on the receptacle.

3.2. Pathogen Isolation and Characterization

A total of 16 strains were isolated from the diseased bracts, of which 14 were successfully purified. After 7 days of culture, all 14 isolates exhibited consistent colony growth and identical colony morphology. The colonies exhibited a characteristic white and fluffy morphology (Figure 2a,b). A light pink coloration was observed on the underside of the plate, which turned gray after 7 days of culture. Aerial hyphae were visible after 36 h of incubation, characterized by highly branched filaments with conidiophores forming at the apex of the branches. Conidia produced on the conidiophores were oval or ellipsoidal in shape, lacking septa, with an average size ranging from 12.6 to 22.5 µm in length and from 3.6 to 6.3 µm in width (Figure 2c,d). Based on both colony and conidia morphology, the isolates were tentatively identified as *Fusarium* sp. [25]. However, sickle-shaped large conidia were rarely observed on the PDA medium.

3.3. Pathogen Identification Molecularly

To specifically identify the isolate, PCR was conducted using fungal universal primers ITS (ITS1/ITS4), as well as *Fusarium*-specific primers Tef-1α (EF1/EF2) and RPB1 (rpb1-Fα/rpb1-G2R). The resulting amplicons were 520 bp, 682 bp, and 1227 bp, respectively, and were subsequently sequenced and queried against GenBank. All 14 isolates had identical sequencing results. The analysis revealed that the ITS region sequence representing isolate RH-2 exhibited high similarity (ranging from 98.84% to 99.22%) with the sequences of *Fusarium verticillioides* and *Gibberella* sp. (Table 3). The ITS sequences were deposited in GenBank and assigned with accession number OP020562. The sequences obtained from the EF1/EF2 primers showed 98.44% to 98.63% identity with the retrieved sequence of *F. verticillioides* from Genbank (Accession No. OQ948493.1, KU372144.1, OQ957222.1, etc.)

However, the sequences obtained from rpb1-Fα /rpb1-G2R primers showed 100% identity with *F. verticillioides* sequences (Table 3). Based on the alignment results of the sequence, we confirmed the identity of the isolate as *F. verticillioides*.

Table 3. Blast results of ITS, Tef-1a, and rpb1 sequence of isolates within Genbank.

Sequencing Primers	Description	Scientific Name	Max Score	Total Score	Query Cover	Per. Ident	Acc.Len	Accession
Internal transcribed spacer 1 (ITS-1) gene	Fusarium verticillioides isolate CYQ007	*F. verticillioides*	922	922	99%	98.84%	522	ON565434.1
	Gibberella fujikuroi isolate m8	Gibberella. sp	920	920	99%	98.84%	660	MW405885.1
	Fusarium verticillioides isolate s10	*F. verticillioides*	920	920	99%	98.84%	578	MW405886.1
	Fusarium verticillioides isolate MRRS1	*F. verticillioides*	918	918	97%	99.22%	517	OQ363325.1
	Fusarium verticillioides isolate ZC1-16	*F. verticillioides*	917	917	99%	98.84%	520	OR884160.1
Translation glongation factor 1-alpha gene(Tef-1α)	Fusarium verticillioides isolate FUG _6	*F. verticillioides*	904	904	99%	98.63%	712	OQ957222.1
	Fusarium verticillioides isolate FB _8	*F. verticillioides*	904	904	100%	98.44%	614	KU372144.1
	Fusarium verticillioides isolate A293	*F. verticillioides*	904	904	100%	98.44%	631	OQ948493.1
	Fusarium verticillioides isolate CN125A2	*F. verticillioides*	904	904	100%	98.44%	593	ON602014.1
	Fusarium verticillioides isolate XC26	*F. verticillioides*	904	904	100%	98.44%	657	ON649853.1
DNA-directed RNA polymerase II largest subunit (rpb1)gene	Fusarium verticillioides strain NRRL 22172	*F. verticillioides*	1749	1749	100%	100%	1555	MN242935.1
	Fusarium verticillioides strain AmP10	*F. verticillioides*	1749	1749	100%	100%	1526	OR841329.1
	Fusarium verticillioides strain LY1306-6	*F. verticillioides*	1749	1749	100%	100%	1792	OR178428.1
	Fusarium verticillioides isolate ZCK-1	*F. verticillioides*	1749	1749	100%	100%	1616	ON692996.1
	Fusarium verticillioides strain LC13653	*F. verticillioides*	1749	1749	100%	100%	1563	MW024492.1

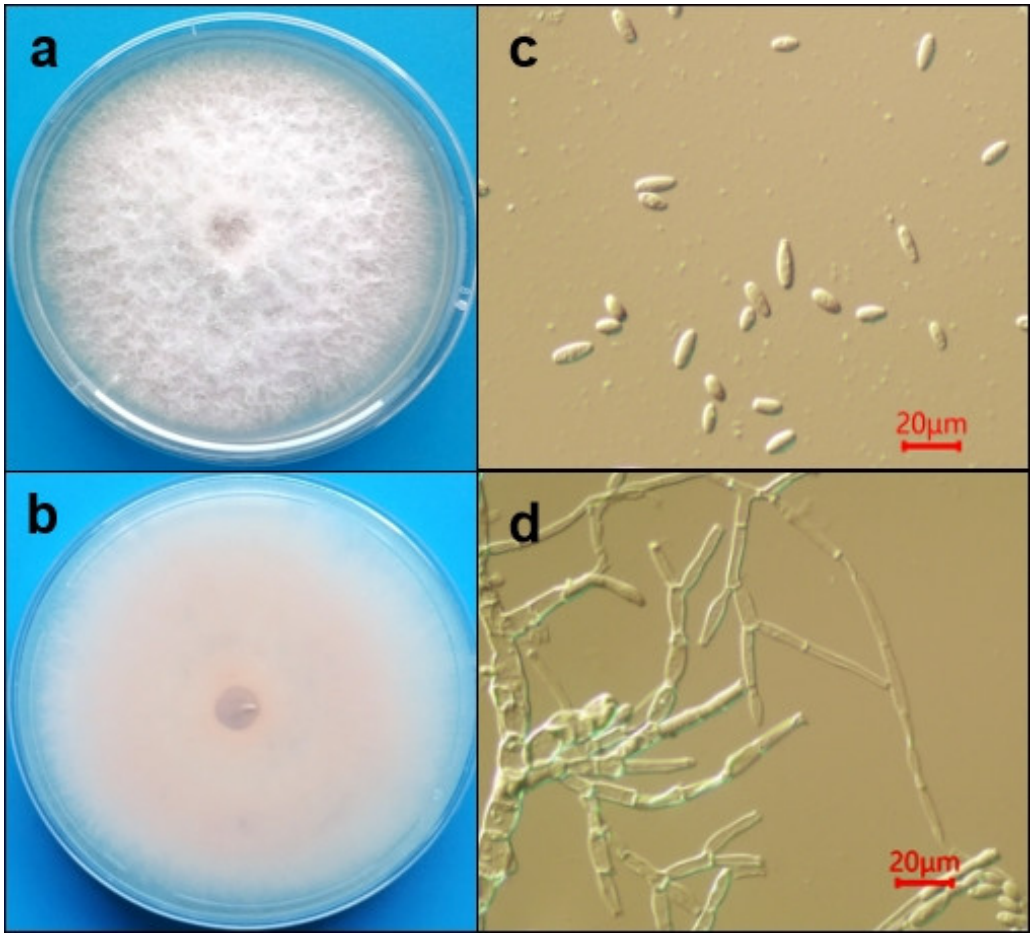

Figure 2. The morphology of the isolates: (**a**) and (**b**) colonies of isolate RH-2 on PDA plates; (**c**) conidium of isolates RH-2; (**d**) mycelium of isolate RH-2. Bar = 20 μm.

3.4. Phylogenetic Analyses

We conducted a multigene analysis and constructed a phylogenetic tree using amplicon sequences obtained via *Fusarium*-specific primers EF1/EF2 and RPB1-Fa/RPB1-G2R. We also retrieved the sequences of different species within the *Fusarium* genera from the NCBI (Figure 3), and *Verticillium dahliae* strains (GU461623) taken alone served as outgroup members. Upon examination of the clustering tree, it became apparent that the isolated strain was clustered into the same clade together with the other three strains of *F. verticillioides* (MW401964, KC808228, and JF740741). This clustering was consistent with our previous identifications and provided accurate confirmation of the species of isolate.

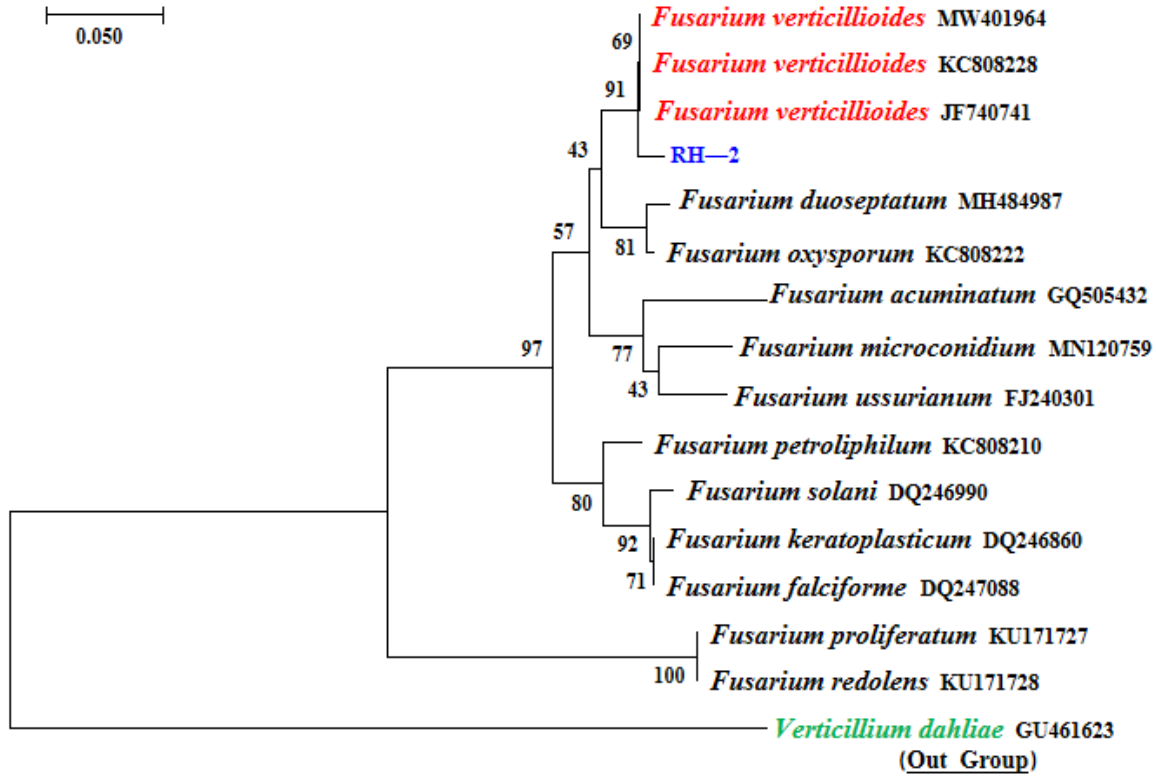

Figure 3. A phylogenetic tree was constructed using multi-gene analysis based on the TEF-1α+ RPB1 primers. The selected strains are marked as RH-2.

3.5. Pathogenicity Identification

To confirm the pathogenicity of isolate RH-2, a conidial suspension was inoculated onto sunflower leaves. Lesions were observed after 2 days post-inoculation (dpi), with the appearance of white to gray mold (mycelium) at the inoculation site by 3 dpi, while no symptoms were noted at the control site (Figure 4a). Stem inoculation resulted in the vertical expansion of lesions along the epidermal layer of the stem at the infection sites (Figure 4b). Inoculation of conidia in the roots led to basal stem darkening to brown, with basal stem constriction observed after 15 dpi. The sunflower leaves exhibited yellowing, and plant height was significantly reduced compared to the control. In severe cases, the inoculated plants were easily uprooted due to root rot (Figure 4c). Inoculation of the conidial suspension onto the bracts of the flower disk at the R5 stage in the field resulted in the appearance of brownish lesions at the bract margins after 7 dpi. Lesions also developed at the infection site on the backside of the flower disk. Flower disk rot was observed during the R7 stage with high humidity (Figure 4e,f). Additionally, browning was observed on small bracts (Figure 4g).

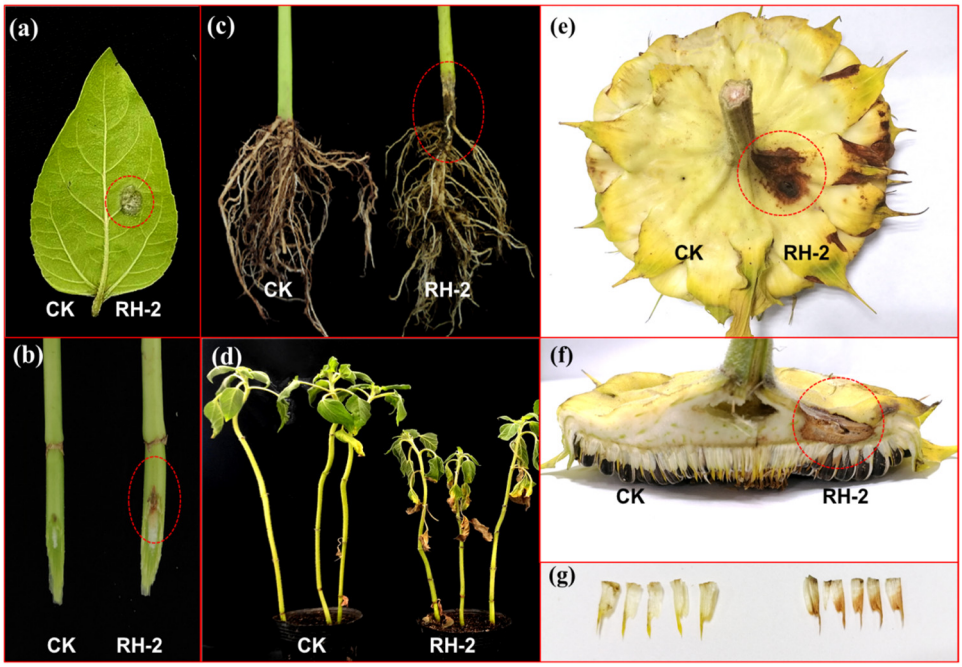

Figure 4. Pathogenicity assessment of isolate RH-2. (**a**) Lesions at the infection site with white to gray mold; (**b**,**c**) pathogenicity of isolate RH-2 on the sunflower leaf, stem, and root. (**d**) Effects of RH-2 infection on plant height. (**e**,**f**) Pathogenicity of isolate RH-2 on the backside of the receptacle. (**g**) Pathogenicity of isolate RH-2 on the bract.

3.6. Pathogen Reisolation

Due to the infection on both the bract and also the back side of the flower disk, this raises the question as to whether the pathogen can also cause seed contamination of the sunflower. To verify the hypothesis, we re-isolated the strain from both the infection site and also the seed coat. Just as we expected, the morphology of the isolated strain was completely the same as the inoculated one (Figure 5a). To verify if the sunflower seeds can also be contaminated by the inoculated strain, we harvested the seeds from 1/8 of the flower disk (Figure 5b), where the lesion formed on the backside of the flower disk. To our surprise, besides the inoculate strain *F. verticillioides*, the other four fungi, namely *Mucorcir cinelloide*, *Cladosporium cladosporioides*, *Rhizopus oryzare*, and *Alternaria* spp., were also obtained from the seed coats of the harvested sunflower seeds (Figure 5a). The average isolation frequency of *F. verticillioides* from the sunflower seeds was 16.9% (Figure 5c).

3.7. Fungicides Sensitivity of F. verticillioides

The inhibitory effects of the selected fungicides on *F. verticillioides* revealed that all tested fungicides could inhibit its growth, although the degree of inhibition varied among the different concentrations of the fungicides (Table 4). As the dilution ratio of the fungicide increased, the colony diameters of *F. verticillioides* also increased. The most significant inhibitory effects were observed with the addition of 280 μg/mL of Tebuconazole·dimetachlone and 128 μg/mL of Pyraclostrobine in the medium, resulting in inhibition rates of 86.54% and 84.16%, respectively. This was followed by Flutolanil (160 μg/mL) and Fludioxonil (5 μg/mL) which had the same inhibition rate of 76.39%. However, the inhibitory effects of Iprodione (500 μg/mL) and Hymexazol (32 μg/mL) were relatively weak, with inhibition rates of only 59.11% and 49.88%, respectively.

Regarding the EC50 values, the tested fungicides exhibited varying levels of sensitivity, with Flutolanil being the most sensitive toward *F. verticillioides*, displaying an EC50 value of only 0.05 μg/mL (R = 0.9825). This was followed by Fludioxonil and Pyraclostrobine, with EC50 values of 0.96 μg/mL (R = 0.9964) and 8.44 μg/mL (R = 0.9907), respectively. Conversely, Iprodione showed the highest EC50 value of 186.21 μg/mL (R = 0.9919). These

results suggest that Fludioxonil, Flutolanil, and Hymexazol could be the most effective candidates for controlling *F. verticillioides*.

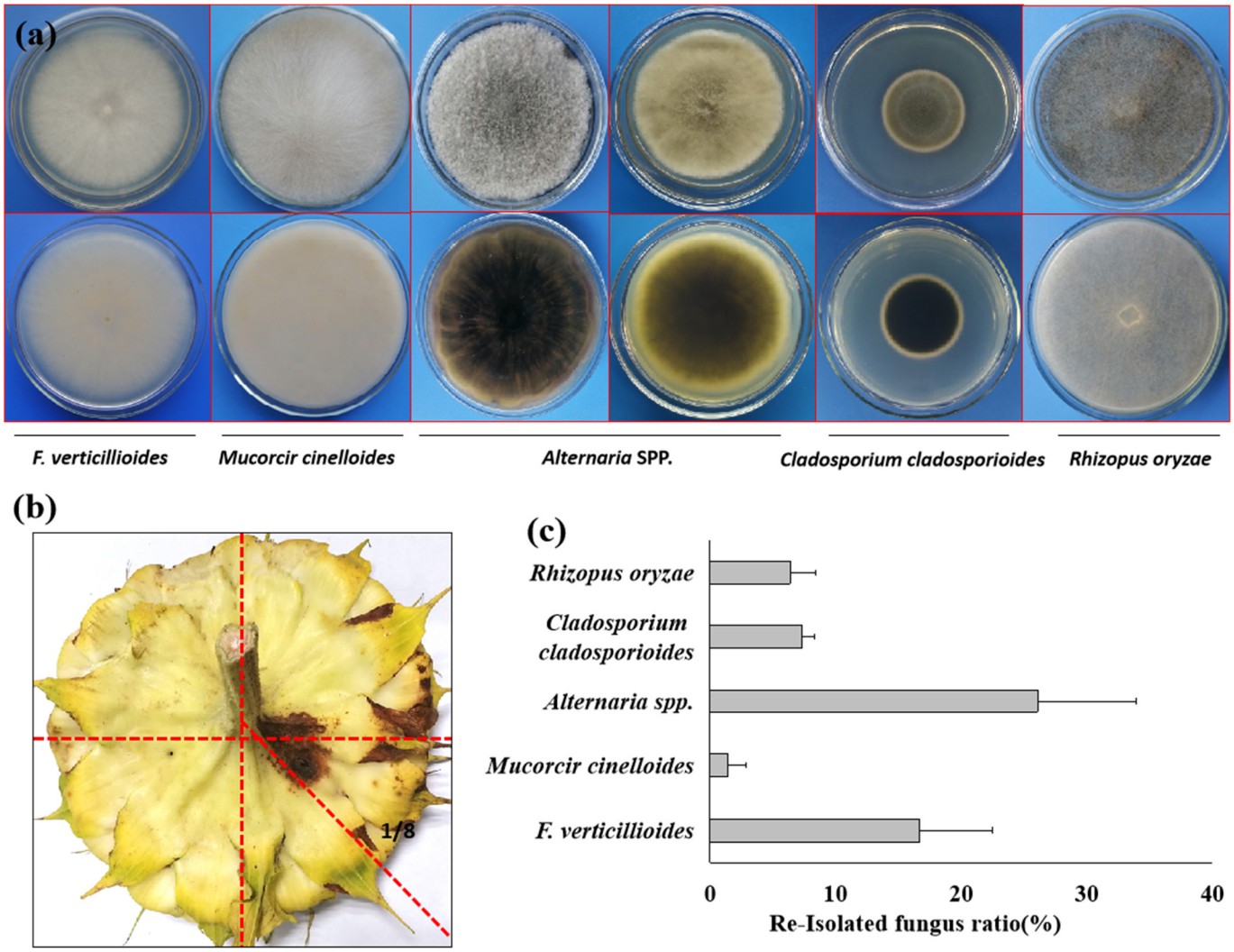

Figure 5. Re-isolation of fungi on seeds. (**a**) Morphological characteristics of the fungus; (**b**) cutting receptacle method for fungal isolation on seeds; (**c**) isolation ratio of fungus.

Table 4. Sensitivity comparison of six fungicides on *F. verticillioides*.

Drug Name	Treatment Concentration (μg/Ml)	Concentration Logarithm (x)	Inhibition Rate %	Probability Value (Y)	Virulence Regression Equation	EC50 (μg/mL)	R
Tebuconazole · dimetachlone	280.00	2.45	86.54	6.10	y = 1.3549x + 2.7613	45.23	0.9972
	140.00	2.15	74.84	5.67			
	70.00	1.85	58.21	5.21			
	35.00	1.54	43.97	4.85			
	17.50	1.24	30.02	4.48			
Pyraclostrobine	128.00	2.11	84.16	6.00	y = 0.8295x + 4.2317	8.44	0.9907
	64.00	1.81	75.77	5.70			
	32.00	1.51	68.83	5.49			
	16.00	1.20	58.61	5.22			
	8.00	0.90	49.72	4.99			

Table 4. *Cont.*

Drug Name	Treatment Concentration (μg/Ml)	Concentration Logarithm (x)	Inhibition Rate %	Probability Value (Y)	Virulence Regression Equation	EC50 (μg/mL)	R
Iprodione	500.00	2.70	59.11	5.23	y =0.5142x + 3.8324	186.21	0.9919
	250.00	2.40	52.35	5.06			
	125.00	2.10	46.72	4.92			
	62.50	1.80	39.02	4.72			
	31.25	1.49	35.39	4.63			
Hymexazol	32.00	1.51	49.88	5.00	y =0.7380x + 3.9027	30.68	0.9943
	16.00	1.20	42.11	4.80			
	8.00	0.90	33.33	4.57			
	4.00	0.60	26.95	4.39			
	2.00	0.30	18.24	4.09			
Flutolanil	160.00	2.20	76.39	5.72	y =0.3252x + 5.0058	0.96	0.9964
	80.00	1.90	73.60	5.63			
	40.00	1.60	69.78	5.52			
	20.00	1.30	67.07	5.44			
	10.00	1.00	62.71	5.32			
Fludioxonil	5.00	0.70	76.39	5.72	y =0.3519x + 5.4496	0.05	0.9825
	1.00	0.00	65.75	5.41			
	0.20	−0.70	59.30	5.24			
	0.05	−1.30	48.74	4.97			
	0.01	−2.00	40.45	4.76			

4. Discussion

Sunflower disk rot (SDR) is attributable to a variety of pathogens. Notably, *Rhizopus stolonifer*/R. oryzae (syn. *R. arrhizus*) and *R. microsporus* are known to induce Rhizopus head rot [6,7], while *Sclerotinia sclerotiorum* is responsible for Sclerotinia head rot [8]. These pathogens substantially affect sunflower seed quality and yield. Botrytis head rot, caused by the ubiquitous fungus *Botrytis cinerea*, is distinguished from Rhizopus head rot by the characteristic gray "fuzz" on the heads due to mycelium and spores [26]. In contrast, bacterial head rot caused by *Erwinia carotovora* is rare and is marked by a slimy, wet, brownish rot of the head without fungal growth or spores, often accompanied by a putrid odor [27].

In our study, we identified a novel pathogen, *F. verticillioides*, as the causative agent of Fusarium head rot via Koch's postulates. The symptoms of SDR differ from those caused by *S. sclerotirum*, where the rotted flower disk easily falls off. SDR caused the tissue to rot around the infection sites only under conditions of high precipitation, with the pathogen capable of spreading from the infected bract to the other part of the flower disk and even leading to seed rot. Remarkably, the pathogen isolated from the flower disk not only infects the flower disk but also affects leaves, stems, and roots, aligning with reports on wheat [28], maize [29], soybean [30], tobacco [9], and sugar beet [31] in China, indicating that *F. verticillioides* can cause root rot in various hosts.

Generally, information regarding the diversity of *Fusarium* spp. associated with commercially cultivated *Helianthus annuus* L. and the potential diseases they cause are limited. There have been reports of various *Fusarium* species causing sunflower wilt, starting with *Fusarium* infestation on the roots and progressing to the stems via the vascular system, ultimately leading to total plant wilting. Numerous *Fusarium* species responsible for sunflower wilt have been identified globally, including *F. oxysporum* f. sp. *helianthi* [32], *F. solani* [33], *F. equiseti*, and *F. culmorum* [34]. However, *F. moniliforme* primarily causes yellowing and discoloration of the leaves and drooping, without inducing root rot [35]. Additionally, *F. tabacinum* [36] can infect sunflower stems, making them prone to breaking at the infection site. Root rot diseases remain the most significant threat to sunflower health.

F. verticillioides has also been reported to cause damping-off in sunflowers in Brazil [37], indicating that *Fusarium* infections are prevalent in sunflower-growing regions worldwide. Previous reports suggest that *Fusarium* can impact sunflower roots via infection of both the vascular system and the epidermal layer. Additionally, sunflower seeds can be contaminated by *Fusarium* spp. as well as other pathogens such as *V. dahliae*, *Alternaria* spp., and *Rhizopus* spp. [23]. In our study, we tested seed contamination from infection sites of flower disks and found that, besides *F. verticillioides*, several other fungi could also colonize the seed coats of sunflowers. This suggests that seed transmission may be a primary source for the occurrence of SDR.

However, the exact preliminary infection sources of SDR remain a question mark. We hypothesize that conidia formed on the diseased basal stems of sunflowers may serve as the re-infection source of SDR. The infection does not appear to be systemic, but it is likely caused by conidia. Therefore, coating sunflower seeds with fungicides such as Fludioxonil, Flutolanil, and Hymexazol is crucial for controlling not only sunflower wilt caused by *Fusarium* spp. but also SDR, thereby keeping the seed clean and maintaining good quality.

This study provides the report of SDR caused by *F. verticillioides* in China. Additionally, the study screened six fungicides for efficiency against the causal agent, with Fludioxonil and Flutolanil proving to be the most effective. This study alerts sunflower research scientists to include SDR in the disease list and provides guidance on successfully controlling the disease using integrated management strategies. Our findings not only expand the known disease list for sunflowers in China but also emphasize the importance for sunflower breeders to develop new varieties resistant to *Fusarium* spp.

Author Contributions: Conceptualization, J.Y. and J.Z. (Jun Zhao); methodology, J.Y., S.S. and H.L.; software, H.L. and W.Z.; validation, Y.W., M.E.A., and J.Z. (Jun Zhao); formal analysis, J.Y. and W.Z.; investigation, J.Y., Y.W., S.S., H.L. and J.Z. (Jun Zhao); resources, Y.W. and J.Z. (Jian Zhang); data curation, S.S., H.L. and W.Z.; writing—original draft preparation, J.Y. and M.E.A.; writing—review and editing, J.Y., Y.W. and J.Z. (Jun Zhao); visualization, Y.W., S.S. and J.Z. (Jian Zhang); supervision, Y.W. and J.Z. (Jun Zhao); project administration, Y.W., J.Z. (Jian Zhang) and J.Z. (Jun Zhao); funding acquisition, Y.W., J.Z. (Jian Zhang) and J.Z. (Jun Zhao). All authors have read and agreed to the published version of the manuscript.

Funding: This research was funded by Basic Research Funds of Inner Mongolia Agricultural University (BR22-13-09); Support Funds of Inner Mongolia Higher University Innovation Team (NMGIRT2320); China Agricultural Research System (CARS-14);The project is supported by Inner Mongolia Science & Technology Plan (2022JBGS0010) and Central Guided Local Science and Technology Development Funds (2022ZY0075).

Data Availability Statement: The original contributions presented in the study are included in the article; further inquiries can be directed to the corresponding author.

Conflicts of Interest: All authors declare no conflicts of interest. We confirm that we have no financial or personal relationships with other individuals or organizations that could have inappropriately influenced our work. There is no professional or personal interest in any product, service, or company that could be construed as influencing the content or review of the manuscript.

References

1. Jockovic, M.; Cveji, S.; Joci, S.; Jeromela, A.M.; Radic, V. Evaluation of sunflower hybrids in multi-environment trial (met). *Turk. J. Field Crops* **2019**, *24*, 202–210. [CrossRef]
2. Guo, S.C.; LI, S.P.; Sun, R.F. Analysis of the overall development of sunflower industry in the world and China. *China Seed Ind.* **2021**, 10–13. (In Chinese) [CrossRef]
3. Zhu, K.Y.; Han, S.C.; Zhao, R.; Wen, Y.J.; Hu, H.C.; Qiao, Y.M.; Lu, J.F.; Cao, K.; Xu, Z.H.; Bao, H.Z.; et al. Current situation and prospects of sunflower production and consumption in China. *Agric. Outlook* **2023**, *19*, 64–71. (In Chinese)
4. Kim, J.H.; Joen, Y.H.; Kim, S.G.; Kim, Y.H. First report on bacterial soft rot of graftcactus chamaecereus silvestrii caused by *pectobacterium carotovorum* subsp. *carotovorum in korea. Plant Pathol. J.* **2007**, *23*, 314–317. [CrossRef]
5. Bauftauf, K.K.; Hekimhan, H.; Maden, S.; Tufr, M. First report of bacterial stalk and head rot disease caused by *pectobacterium atrosepticum* on sunflower in turkey. *Plant Dis.* **2009**, *93*, 1352.

6. Rasera, K.; Osório, N.M.; Mitchell, D.A.; Krieger, N.; Ferreira-Dias, S. Interesterification of fat blends using a fermented solid with lipolytic activity. *J. Mol. Catal. B Enzym.* **2002**, *76*, 75–81. [CrossRef]
7. Mathew, F.M.; Prasifka, J.R.; Gaimari, S.D.; Shi, L.; Gulya, T.J. *Rhizopus oryzae* associated with melanagromyza splendida and stem disease of sunflowers (*helianthus annuus*) in california. *Plant Health Prog.* **2015**, *16*, 39–42. [CrossRef]
8. Gregoire, T.; Lamey, A.; Hofman, V. Sclerotinia head rot of sunflower. *Magn. Reson. Imaging Clin. N. Am.* **2010**, *21*, 6–18.
9. Gai, X.T.; Jiang, N.; Lu, C.H.; Xia, Z.Y.; He, Y.S. First report of tobacco fusarium root rot caused by *Fusarium verticillioides* in china. *Am. Phytopathol. Soc.* **2021**. [CrossRef]
10. Chen, X.; Liu, D.; Zhang, Y.; Qin, Z.; Zhou, X. Isolation and identification of *fusarium* from cucumber wilt plants. *J. Northeast Agric. Univ.* **2010**, *41*, 37–44. [CrossRef]
11. Moreira, S.I.; Melo, M.P.; Andrade, C.C.L.; Alves, E.; Pereira, O.L. Postharvest ginger rhizome rot caused by *Fusarium verticillioides* in brazil. *Plant Dis.* **2015**, *99*, 1177. [CrossRef]
12. An, Y.N.; Murugesan, C.; Choi, H.; Kim, K.D.; Chun, S.C. Current Studies on Bakanae Disease in Rice: Host Range, Molecular Identification, and Disease Management. *Mycobiology* **2023**, *51*, 195–209. [CrossRef] [PubMed]
13. Borah, S.N.; Deka, S.; Sarma, H.K. First report of *Fusarium verticillioides* causing stalk rot of maize in assam, india. *Plant Dis.* **2016**, *100*, 1501. [CrossRef]
14. Dastjerdi, R.; Karlovsky, P. Systemic infection of maize, sorghum, rice, and beet seedlings with fumonisin-producing and nonproducing *Fusarium verticillioides* strains. *Plant Pathol. J.* **2015**, *31*, 334–342. [CrossRef] [PubMed]
15. Tahat, M.M.; Aldakil, H.; Alananbeh, K.; Salem, N.M. First Report of *Fusarium verticillioides* Causing Fusarium Ear Rot of Corn in Jordan. *Plant Dis.* **2022**. *online ahead of print*. [CrossRef] [PubMed]
16. Mehl, O.H.L. Fusarium hardlock associated with *Lygus lineolaris* (hemiptera: Miridae) injury in southeastern cotton. *Plant Dis.* **2021**, *105*, 53–59.
17. Doyle, J.J.; Doyle, J.L. lsolation of plant DNA from fresh tissue. *Focus* **1990**, *12*, 39–40.
18. White, T.J.; Bruns, T.; Lee, S.J.W.T.; Taylor, J. Amplification and direct sequencing of fungal ribosomal RNA genes for phylogenetics. *PCR Protocl. Guide Methods Appl.* **1990**, *18*, 315–322.
19. O'Donnell, K.; Kistler, H.C.; Cigelnik, E.; Ploetz, R.C. Multiple evolutionary origins of the fungus causing Panama disease of banana: Concordant evidence from nuclear and mitochondrial gene genealogies. *Proc. Natl. Acad. Sci. USA* **1998**, *95*, 2044–2049. [CrossRef]
20. Yan, M.G. Species diversity study and new species identification of endophytic *Fusarium oxysporum* in Longblood tree of Yunnan. Master's Thesis, Yunnan University, Kunming, China, 2022. (In Chinese) [CrossRef]
21. Kumar, S.; Stecher, G.; Tamura, K. MEGA7: Molecular evolutionary genetics analysis version 7.0 for bigger datasets. *Mol. Biol. Evol.* **2016**, *33*, 1870–1874. [CrossRef]
22. Chen, Y.; Li, H.; Chen, C.; Zhou, M. Sensitivity of *Fusarium graminearum* to fungicide js399-19: In vitro determination of baseline sensitivity and the risk of developing fungicide resistance. *Phytoparasitica* **2008**, *36*, 326–337. [CrossRef]
23. Addrah, M.E.; Zhang, Y.; Zhang, J.; Liu, L.; Zhou, H.; Chen, W.; Zhao, J. Fungicide Treatments to Control Seed-borne Fungi of Sunflower Seeds. *Pathogens* **2019**, *9*, 29. [CrossRef] [PubMed]
24. Zhou, M.G.; Ye, Z.Y.; Liu, J.F. Progress of fungicide resistance. *J. Nanjing Agric. Univ.* **1994**, *17*, 33–41.
25. Leslie, J.F.; Summerell, B.A. *The Fusarium Laboratory Manual II A Brief History of Fusarium Taxonomy*; Blackwell Publishing: Hoboken, NJ, USA, 2006. [CrossRef]
26. Zhao, Y.; Wang, Z.J.; Wang, C.B.; Tan, B.Y.; Luo, X.D. New and Antifungal Diterpenoids of Sunflower against Gray Mold. *J. Agric. Food Chem.* **2023**, *71*, 16647–16656. [CrossRef] [PubMed]
27. Custers, J.H.; Harrison, S.J.; Sela-Buurlage, M.B.; van Deventer, E.; Lageweg, W.; Howe, P.W.; van der Meijs, P.J.; Ponstein, A.S.; Simons, B.H.; Melchers, L.S.; et al. Isolation and characterisation of a class of carbohydrate oxidases from higher plants, with a role in active defence. *Plant J.* **2004**, *39*, 147–160. [CrossRef]
28. Dong, F.; Li, Y.; Chen, X.; Wu, J.; Wang, S.; Zhang, X.; Ma, G.; Lee, Y.W.; Mokoena, M.P.; Olaniran, A.O.; et al. Analysis of the *Fusarium graminearum* species complex from gramineous weeds near wheat fields in Jiangsu Province, China. *Plant Dis.* **2021**, *105*, 3269–3275. [CrossRef]
29. Gai, X.T.; Xuan, Y.H.; Gao, Z.G. Diversity and pathogenicity of *Fusarium graminearum* species complex from maize stalk and ear rot strains in northeast China. *Plant Pathol.* **2017**, *66*, 1267–1275. [CrossRef]
30. Chang, X.; Dai, H.; Wang, D.; Zhou, H.; He, W.; Fu, Y.; Ibrahim, F.; Zhou, Y.; Gong, G.; Shang, J.; et al. Identification of *Fusarium* species associated with soybean root rot in Sichuan Province, China. *Eur. J. Plant Pathol.* **2018**, *151*, 563–577. [CrossRef]
31. Cao, S.; Yang, N.; Zhao, C.; Liu, J.; Han, C.; Wu, X. Diversity of *Fusarium* species associated with root rot of sugar beet in China. *J. Gen. Plant Pathol.* **2018**, *84*, 321–329. [CrossRef]
32. El Mahjoub, M. Vascular fusarium wilt of sunflower in Tunisia caused by *Fusarium oxysporum* (Sn. et H.) F. sp. *helianthi* nov. sp. [French]. *Ann. De L'institut Natl. De La Rech. Agron. De Tunis.* **1975**, *48*, 3–11.
33. Haggag, W.M.; Amin, A.W. Efficiency of trichoderma species on control of Fusarium rot, root knot and reniform nematodes disease complex on sunflower. *Pak. J. Biol. Sci.* **2001**, *4*, 679–683. [CrossRef]
34. Pineda, P.J.B.; Avila, M.J.M. Management and control of sunflower disease in Portuguesa State. *FONAIAP Divulg.* **1991**, *9*, 6–8.
35. Bhargava, S.N.; Shukla, D.N.; Singh, N. Wilt of sunflower caused by *Fusarium moniliforme*. *Indian Phytopathol.* **1978**, *31*, 382–383.

36. Zazzerini, A. New sunflower disease caused by *Fusarium tabacinum*. *Plant Dis.* **1987**, *71*, 1043–1104. [CrossRef]
37. Pozzi, C.R.; Braghini, R.; Arcaro, J.R.; Zorzete, P.; Israel, A.L.; Pozar, I.O.; Denucci, S.; Corrêa, B. Mycoflora and occurrence of alternariol and alternariol monomethyl ether in Brazilian sunflower from sowing to harvest. *J. Agric. Food Chem.* **2005**, *53*, 5824–5828. [CrossRef]

Disclaimer/Publisher's Note: The statements, opinions and data contained in all publications are solely those of the individual author(s) and contributor(s) and not of MDPI and/or the editor(s). MDPI and/or the editor(s) disclaim responsibility for any injury to people or property resulting from any ideas, methods, instructions or products referred to in the content.